

Multisoliton ejection from an amplifying potential trap

Assaf Barak,¹ Or Peleg,¹ Avy Soffer,² and Mordechai Segev¹

¹Physics Department and Solid State Institute, Technion, Haifa 3200, Israel

²Department of Mathematics, Rutgers University, New Brunswick, New Jersey 08903, USA

Received April 21, 2008; revised June 8, 2008; accepted June 17, 2008;
posted July 7, 2008 (Doc. ID 95263); published August 5, 2008

We study theoretically the dynamics of a beam launched inside an amplifying trap potential. Raising the amplification transforms the dynamics from linear tunneling at low amplification to periodic ejection of a sequence of identical solitons (when the amplification rate exceeds the tunneling rate) and, at strong amplification, to nonperiodic multisoliton ejection. © 2008 Optical Society of America

OCIS codes: 190.6135, 190.4420.

Controlled emission of solitons from waveguides and through potential barriers has been investigated since the late 1980s [1,2]. The phenomenon was observed years later, for a waveguide with asymmetric nonlinear cladding [3] and for a quadratic nonlinear waveguide with a phase-mismatched boundary [4]. Recent work [5] has suggested that matter-wave solitons could be emitted from a potential trap via a linear tunneling process. The power that tunnels through the potential barrier accumulates outside the trap and forms a bright soliton. In a similar vein, nonlinear transmission of matter-wave solitons through linear and nonlinear inhomogeneities was suggested [6]. These phenomena were recently observed [7] with optical spatial solitons launched into a trap potential embedded in a nonlinear medium. It was shown [7] that the dynamics of a beam launched into a potential trap changes dramatically as a function of the initial beam power, transforming from linear to soliton tunneling and eventually to soliton ejection. The diversity of effects displayed by a wave function in a potential trap embedded in a nonlinear medium becomes even richer when gain is introduced. In optics the combination of amplification and nonlinearity, in conjunction with solitons, leads to fascinating phenomena such as solitons in parametric oscillators [8], solitons in the complex Ginzburg–Landau equation (CGLE) [9], “optical similaritons” (self-similar pulses in amplifiers) [10], solitons in *PT* periodic potentials [11], and more. Also, it was recently predicted that solitons are emitted from an amplifying layer on the surface of a periodic structure [12].

Here, we study the dynamics of a low-power beam launched into an amplifying trap potential. At weak amplification the beam tunnels linearly from the trap. When the amplification rate exceeds the tunneling rate, a periodic sequence of identical solitons is ejected from the trap. Finally, at strong amplification, the multisoliton ejection process becomes nonperiodic. The system can be realized in photorefractive materials, where the potential structure is induced by light [7,13,14] and the amplification is achieved via two-wave mixing.

The propagation of a paraxial monochromatic beam launched into an amplifying potential trap em-

bedded in a medium with saturable nonlinearity is described by the (1+1)*D* NLSE [15]

$$i\frac{\partial\psi}{\partial z} + \frac{\partial^2\psi}{\partial x^2} - \frac{1}{1 + I_{\text{POT}} + |\psi|^2}\psi - ig\psi = 0, \quad (1)$$

where z and x are the normalized coordinates, ψ is the field envelope, I_{POT} is the intensity inducing the trap potential ($|\psi|^2$ and I_{POT} are normalized to the background illumination), and g is a spatially dependent gain coefficient. The gain is taken to be saturable: $g = g_0(x)/(1 + q|\psi|^2)$, where $g_0(x)$ determines the amplifying layer profile, $g_0(0)$ is the maximal gain, and q determines the saturation strength. At low intensity (when the dynamics is governed by linear effects), the gain can be Taylor expanded: for $q|\psi|^2 \ll 1$, $g \approx g_0(x)(1 - q|\psi|^2)$. Substituting g into Eq. (1) leads to the CGLE with a saturable nonlinearity,

$$i\frac{\partial\psi}{\partial z} + \frac{\partial^2\psi}{\partial x^2} - \frac{1}{1 + I_{\text{POT}} + |\psi|^2}\psi - ig_0(x)\psi + ig_0(x)q|\psi|^2\psi = 0. \quad (2)$$

In this limit power tunnels linearly through the barrier. In the absence of amplification the field in the trap decays exponentially [7], with a decay rate α inversely proportional to the tunneling distance $Z_{\text{tun}} = 1/\alpha$, (Z_{tun} is equivalent to tunneling time of a particle in a trap). The power of the beam inside the trap is $P = \int_{-L}^L |\psi|^2 dx$, where $2L$ is the trap width [Fig. 1(a)]. P varies according to

$$\frac{\partial P}{\partial z} = \int_{-L}^L g_0(x)|\psi|^2 dx - \int_{-L}^L \alpha|\psi|^2 dx - \int_{-L}^L qg_0(x)|\psi|^4 dx. \quad (3)$$

We use a Gaussian ansatz for the beam profile, $|\psi| = \psi_0 e^{-(x^2/2\sigma_t^2)}$, where ψ_0 and σ_t determine the beam shape [dashed curve in Fig. 1(a)]. For concreteness, we use a Gaussian profile for the amplifying layer: $g_0(x) = g_0(0)e^{-(x^2/\sigma_G^2)}$, where $\sigma_G/\sqrt{2}$ is the amplifying layer width [dotted-dashed curve in Fig. 1(a)]. The beam is amplified only when the rate of amplification exceeds the tunneling loss. When gain and loss are

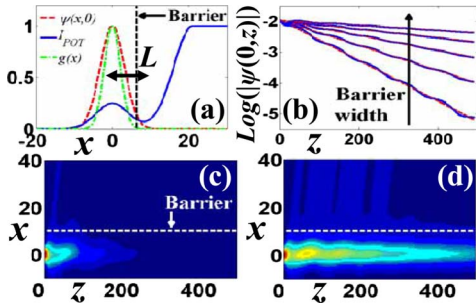


Fig. 1. (Color online) (a) Spatial profiles of the initial wave function (dashed curve) launched into the potential trap, the light inducing the trap potential (solid curve), and the amplifying layer (dashed-dotted curve). (b) Peak amplitude of the field (in logarithmic scale) versus propagation distance z for various barrier widths, without amplification. (c), (d) Propagation of a beam launched at the trap center (c) without amplification [$g_0(0)=0$], and (d) with amplification below the minimal gain for multisoliton ejection [$g_0(0)=0.95g_m$]. Other parameters are $q=1$, $\sigma_G=1.7$, $\sigma_t=4.2$, $\alpha=0.0066$, and $\psi_0=0.16$, which yields $g_m=0.0184$. The dashed line marks the potential barrier. Both beams decay exponentially owing to tunneling loss.

balanced, the beam maintains its power and shape as it propagates. The condition for such a balance is that the rate of change of the beam power is zero, that is, $\partial P/\partial z=0$. By choosing a narrow amplifying layer ($L \approx 6\sigma_G$), and since most of the power of the beam is contained inside the trap ($L \approx 3\sigma_t$), the condition for the gain–loss balance is

$$\frac{g_m}{\alpha} \approx \left(\frac{1}{\sqrt{1+R^2}} - \frac{q\psi_0^2}{\sqrt{2+R^2}} \right)^{-1}, \quad (4)$$

where $R=\sigma_t/\sigma_G$ is proportional to the ratio between the widths of the beam and of the amplifying layer and g_m is the minimal gain [$g_0(0)$] needed for multisoliton ejection.

Numerical simulations of Eq. (1) corroborate these predictions. A Gaussian beam is launched at the center of the trap [solid curve in Fig. 1(a)], with the parameters $q=1$, $\sigma_G=1.7$, $\sigma_t=4.2$, $\alpha=0.0066$ (determined by the profile of the external potential), and $\psi_0=0.16$, which yields $g_m=0.0184$. When $g_0(0)=0$ the field of the beam decays exponentially inside the trap, as shown in Fig. 1(b) for various barrier widths. For a specific width raising, the gain slows the linear decay owing to tunneling, as shown in Figs. 1(c) and 1(d) for gain levels of $g_0(0)=0$ and $g_0(0)=0.95g_m$. The beam in the trap in both figures decays exponentially, although in Fig. 1(c) the decay rate is fast (no amplification), and in Fig. 1(d) it is much slower (amplification below minimum gain for multisoliton ejection). At the minimum gain for multisoliton ejection [$g_0(0)=g_m$], the power loss owing to linear tunneling is exactly balanced by the amplification. Hence, the power in the trap does not change during propagation, although ejection does not occur [Fig. 2(a)]. When the gain is increased beyond the minimal gain for multisoliton ejection, the amplification process overcomes the losses and the power in the trap is amplified during propagation. Analyzing the beam dy-

namics by the effective-particle model for the motion of \bar{x} , the average position of the beam in the x direction [16], yields

$$\frac{d^2\bar{x}}{dz^2} = 2p^{-1} \int_{-\infty}^{\infty} \frac{dF}{dx} |\psi|^2 dx, \quad (5)$$

where $p = \int_{-\infty}^{\infty} |\psi|^2 dx$ is the soliton power and F represents the total refractive index (linear+nonlinear), which does not depend on the amplification (because the amplification, being symmetric in x , does not affect the beam trajectory). Here, $F = -[1/(1+I_{\text{POT}}+|\psi|^2)]$ arising from the saturable nonlinearity and it depends on the soliton profile and on the potential. Equation (5) is written as

$$\frac{d^2\bar{x}}{dz^2} = -\frac{d\varphi(\bar{x})}{d\bar{x}}, \quad (6)$$

where $\varphi(x)$ is the effective potential that the effective particle feels [7]. Since the beam intensity is increasing during propagation, the effective induced potential varies as well. As the beam intensity reaches the ejection threshold [7] the beam overcomes the effective potential barrier and a soliton is ejected. The propagation of a beam with an initial field amplitude of $\psi_0=0.1\psi_{\text{TH}}$ is shown in Figs. 2(b) and 2(c) for $g_0(0)=1.5g_m$ and $2g_m$, respectively. As we increase the gain the intensity of the beam reaches the ejection threshold faster and ejection occurs earlier. Figure 2(d) shows the effective potential for various beam intensities. The effective potential determining the dynamics of the beams in Figs. 2(b) and 2(c) varies with propagation [from the dashed curve, through the solid curve, and to the dashed-dotted curve in Fig. 2(d)] until a soliton is ejected. The only difference between Figs. 2(b) and 2(c) is how soon the ejection process occurs.

As the soliton is ejected from the trap, some power is left behind and experiences amplification. When the amplified intensity of this “leftover” beam reaches the ejection threshold, another soliton (identical to the previous one) is ejected. The power re-

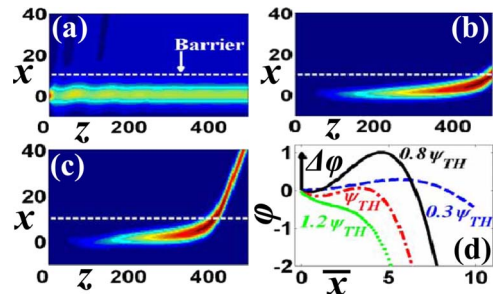


Fig. 2. (Color online) Soliton ejection through an amplifying layer. (a) Propagation of a beam launched at the trap center with (a) $g_0(0)=g_m$ (amplification equal to minimal gain for multisoliton ejection), (b) $g_0(0)=1.5g_m$, (c) $g_0(0)=2g_m$. Other parameters in (a)–(c) are $q=1$, $\sigma_G=1.7$, $\sigma_t=4.2$, $\alpha=0.0066$, and $\psi_0=0.16$, which yields $g_m=0.0184$. (d) Effective induced potential for various beam intensities. $\Delta\varphi$ is the difference between the maximum of the effective induced potential and $\varphi(0)$.

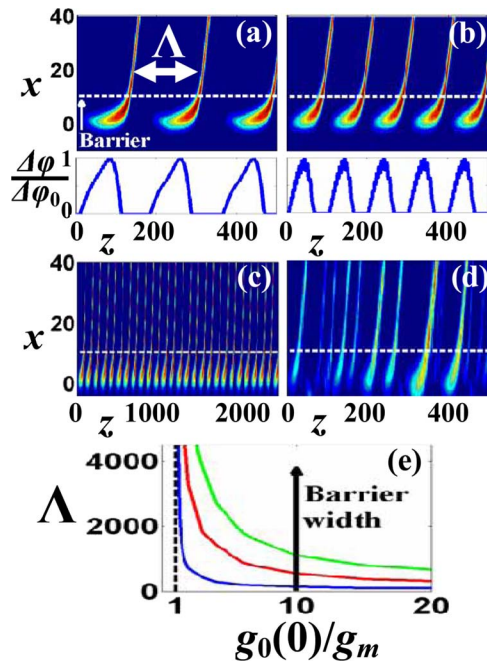


Fig. 3. (Color online) Periodic (a)–(c) and nonperiodic (d) multisoliton ejection. (a) Propagation of a beam launched at the trap center with (a) $g_0(0) = 6g_m$, (b) $g_0(0) = 15g_m$, and normalized $\Delta\varphi$. (c) Long-distance propagation with $g_0(0) = 15g_m$. (d) Beam propagation for $g_0(0) = 50g_m$. At gain levels between minimal gain for multisoliton ejection and $g_0(0) \approx 20g_m$ the process is periodic, whereas at high gain the process is nonperiodic. Other parameters in (a)–(d) are $q=1$, $\sigma_G=1.7$, $\sigma_t=4.2$, $\alpha=0.0066$, and $\psi_0=0.16$, which yields $g_m=0.0184$. (e) Distance between the ejected solitons, Λ , versus gain (normalized to the minimal gain for multisoliton ejection, g_m) for various barrier widths.

maintaining in the trap is again amplified, until a third soliton is ejected, etc. This process is fully periodic, and an infinite number of identical solitons is ejected from the trap [Figs. 3(a)–3(c)]; the latter showing long-distance propagation]. It is obvious from Figs. 3(a) and 3(b) that the soliton is ejected as soon as $\Delta\varphi$, the difference between the maximum of the effective induced potential and $\varphi(0)$, vanishes [$\Delta\varphi$ was defined in Fig. 2(d)]. This process is bounded from above by soliton interactions. As $g_0(0)$ is increased, the distance between the ejected solitons, Λ , decreases [Fig. 3(e)]. When Λ is of the order of the soliton width, the interactions among the solitons destroy the periodicity of the process [Fig. 3(d)]. Figure 3(e) shows Λ versus gain (normalized to g_m) for various barrier widths. As the barrier width is increased, the ejection threshold increases and, therefore, for a given $g_0(0)$ Λ is increasing with the barrier width.

To conclude, we proposed a controlled multisoliton ejection process. The shape of the ejected solitons is predetermined by the shape of the external (linear) potential, and the distance between the solitons is de-

termined by the gain. These results were obtained with nonlinear saturable gain. However, they occur also with linear amplification, as long as the amplification level is low enough for the beam to eject as a soliton before its intensity increases too much and the beam breaks up. The minimum gain needed for multisoliton ejection can also be controlled through “environment engineering” [17,18]. By designing the coupling to the external potential to alter the tunneling rate, or to make it nonexponential, the minimum gain for multisoliton ejection can be reduced. Thus, we achieved a controlled process of multisoliton ejection from a potential trap. These ideas are general and can be implemented in any kind of nonlinear media and with different types of amplification.

This work was supported by the Israel Science Foundation.

References

1. E. M. Wright, G. I. Stegeman, C. T. Seaton, J. V. Moloney, and A. D. Boardman, *Phys. Rev. A* **34**, 4442 (1986).
2. M. A. Gubbels, E. M. Wright, G. I. Stegeman, and C. T. Seaton, *J. Opt. Soc. Am. B* **4**, 1837 (1987).
3. P. Dumais, A. Villeneuve, A. Saher-Helmy, J. S. Aitchison, L. Friedrich, R. A. Fuerst, and G. I. Stegeman, *Opt. Lett.* **25**, 1282 (2000).
4. F. Baronio, C. De Angelis, P. H. Pioger, V. Couderc, A. Barthélémy, Y. Min, V. Quiring, and W. Sohler, *Opt. Lett.* **28**, 2348 (2003).
5. G. Dekel, V. Fleurov, A. Soffer, and C. Stucchio, *Phys. Rev. A* **75**, 043617 (2007).
6. J. Garnier and F. K. Abdullaev, *Phys. Rev. A* **74**, 013604 (2006).
7. A. Barak, O. Peleg, C. Stucchio, A. Soffer, and M. Segev, *Phys. Rev. Lett.* **100**, 153901 (2008).
8. P.-S. Jian, W. E. Torruellas, M. Haelterman, S. Trillo, U. Peschel, and F. Lederer, *Opt. Lett.* **24**, 400 (1999).
9. N. N. Akhmediev, V. V. Afanasjev, and J. M. Soto-Crespo, *Phys. Rev. E* **53**, 1190 (1996).
10. J. M. Dudley, C. Finot, D. J. Richardson, and G. Millot, *Nat. Phys.* **3**, 597 (2007).
11. Z. H. Musslimani, K. G. Makris, R. El-Ganainy, and D. N. Christodoulides, *Phys. Rev. Lett.* **100**, 030402 (2008).
12. Y. V. Kartashov, V. A. Vysloukh, and L. Torner, *Opt. Lett.* **32**, 2061 (2007).
13. N. K. Efremidis, S. M. Sears, D. N. Christodoulides, J. W. Fleischer, and M. Segev, *Phys. Rev. E* **66**, 046602 (2002).
14. J. W. Fleischer, M. Segev, N. K. Efremidis, and D. N. Christodoulides, *Nature* **422**, 147 (2003).
15. M. Segev, M. F. Shih, and G. C. Valley, *J. Opt. Soc. Am. B* **13**, 706 (1996).
16. A. B. Aceves, J. V. Moloney, and A. C. Newell, *Phys. Rev. A* **39**, 1809 (1989).
17. A. G. Kofman and G. Kurizki, *Phys. Rev. Lett.* **87**, 270405 (2001).
18. S. Longhi, *Phys. Rev. Lett.* **97**, 110402 (2006).